Ultra-low field magnetic resonance imaging detection with gradient tensor compensation in urban unshielded environment

Hui Dong, Longqing Qiu, Wen Shi, Baolin Chang, Yang Qiu, Lu Xu, Chao Liu, Yi Zhang, Hans-Joachim Krause, Andreas Offenhäusser, and Xiaoming Xie

Citation: Applied Physics Letters **102**, 102602 (2013); doi: 10.1063/1.4795516
View online: http://dx.doi.org/10.1063/1.4795516
View Table of Contents: http://scitation.aip.org/content/aip/journal/apl/102/10?ver=pdfcov
Published by the AIP Publishing

Ultra-low field magnetic resonance imaging detection with gradient tensor compensation in urban unshielded environment

Hui Dong (董慧),[1,a)] Longqing Qiu (邱隆清),[1,a)] Wen Shi (侍文),[1,a)] Baolin Chang (常宝林),[1,a)] Yang Qiu (邱阳),[1,a)] Lu Xu (徐璐),[1,a)] Chao Liu (刘超),[1,2,a)] Yi Zhang (张懿),[2,a)] Hans-Joachim Krause,[2,a)] Andreas Offenhäusser,[2,a)] and Xiaoming Xie (谢晓明)[1,a),b)]
[1]*State Key Laboratory of Functional Materials for Informatics, Shanghai Institute of Microsystem and Information Technology, Chinese Academy of Sciences (CAS), Shanghai, 200050, China*
[2]*Peter Grünberg Institute(PGI-8), Forschungszentrum Jülich (FZJ), Jülich, D-52425, Germany*

(Received 28 January 2013; accepted 1 March 2013; published online 15 March 2013)

An ultra-low field (ULF) magnetic resonance imaging (MRI) system was set up in an urban laboratory without magnetic shielding. The measured environmental gradient fields of $1 \sim 5\,\mu$T/m caused image distortion. We designed a gradient detection and compensation system to effectively balance the gradient tensor components. The free induction decay signal duration of tap water was thus extended from 0.3 s to 2.5 s, providing the possibility for high-resolution imaging. Two-dimensional MRI images were then obtained at 130 μT with a helium-cooled second-order superconducting quantum interference device gradiometer. This result allows us to develop an inexpensive ULF MRI system for biological studies. © *2013 American Institute of Physics*. [http://dx.doi.org/10.1063/1.4795516]

Ultra-low field (ULF) magnetic resonance imaging (MRI) based on superconducting quantum interference device (SQUID) detection exhibits attractive advantages,[1] such as imaging in the presence of metallic objects,[2] T_1-weighted contrast imaging of tumors without contrast agents,[3] simultaneous functional and structural imaging of the human brain with magnetoencephalography (MEG), MRI,[4] etc. All these results were achieved in a magnetically shielded room (MSR). The drawbacks of a MSR are its high cost and the fact that it is a small closed room.

In order to reduce the system cost and to realize an open system, we set up an ULF MRI system at an urban laboratory without magnetic shielding. In this case, the measurement field (B_m) includes the environmental magnetic field superposed onto the static field (B_0) applied by a Helmholtz coil pair. The time domain fluctuations and the spatial inhomogeneity of the environmental magnetic field thus become the major challenges. We effectively stabilized temporal field fluctuations as strong as 1 μT by the active compensation method.[5] However, the behavior and variation of the spatial gradient tensor[6] which have been well studied in geophysical research need to be elucidated for unshielded ULF MRI detection.

The subject of this paper is a gradient tensor detection and compensation system that we developed for unshielded ULF MRI experiments. The gradient field tensor was measured using six fluxgate magnetometers. Then the measured tensor components were cancelled by six pairs of gradient coils. After optimizing the compensating currents flowing in the coils, 2D MRI was performed.

The nuclear magnetic resonance (NMR) signals and MRI images were recorded by a 2nd order gradiometer (number of turns: 1-2-1, niobium wire diameter: 0.1 mm) which inductively coupled to a liquid-helium-cooled dc SQUID. The diameter and baseline of the gradiometer were 18 mm and 2×40 mm, respectively. The environmental noise spectrum measured by the 2nd order gradiometer exhibited white noise above 5 kHz at the level of 30 fT/$\sqrt{}$Hz. The measurement field B_m was chosen to be 129 μT, corresponding to a ^{1}H Larmor frequency of 5.5 kHz.

The schematic of ULF MRI system built up in our lab is shown in Fig. 1. The vertical component ($B_\perp$) of earth's magnetic field was compensated by a square Helmholtz coil pair (not shown in Fig. 1 for simplicity) and its horizontal component $B_{//}$ is about 29 μT. The applied static field B_0 and the ac pulse field B_{ac} were generated by circular Helmholtz coil pairs set along x and y axis, respectively. The total measurement field B_m of about 129 μT was formed by the superposition of $B_{//}$ and B_0. The 3D gradient fields designed for MRI were produced by a round Maxwell coil pair with a radius of 0.416 m ($G_{xx} = \partial B_x/\partial x$) and two planar gradient coil pairs ($G_{xy} = \partial B_x/\partial y$ & $G_{xz} = \partial B_x/\partial z$) with side lengths of 1.03 m and distance of 0.82 m. The design of our planar coil pair was illustrated by Zhang *et al.*[7] The 10 rectangular coils increase in width from 0.1 m to 0.5 m with a step of 0.1 m on each side, and their number of turns are 18, 14, 10, 6, and 2, respectively. The 0.65 T NdFeB permanent magnet pair providing the prepolarization field B_p was placed 1.5 m away from the cryostat (the measurement position). The yoke made of soft iron surrounding the magnets guides the magnetic field lines and reduces their leakage, therefore improving the field homogeneity at the measurement position. The sample was driven by a commercial electric actuator and automatically transported from the magnet gap to the SQUID detector in 1.4 s after prepolarization of 6 s. Benefits and challenges of this approach as compared to *in-situ* prepolarization were discussed by Liu *et al.*[8] Subsequently, the ac pulse field was applied to tilt the magnetization.

The gradient field in laboratory environment consists of not only the first-order but also the higher order gradient components. For simplicity, we assume that only the first-order components influence the NMR/MRI detection. To evaluate

[a)]Joint Research Laboratory on Superconductivity & Bioelectronics, Collaboration between CAS-Shanghai & FZJ
[b)]Author to whom correspondence should be addressed. Electronic mail: xmxie@mail.sim.ac.cn.

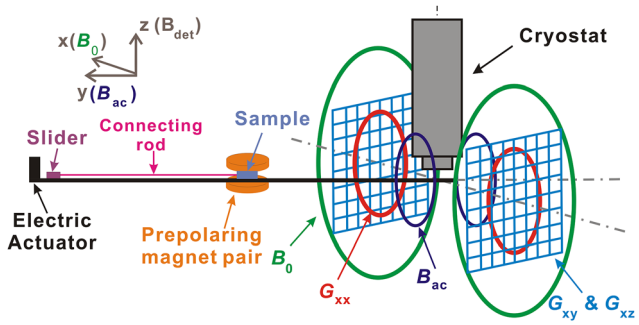

FIG. 1. Schematic of the ULF MRI system.

the first-order gradient field tensor consisting of nine components, a gradient field tensor measurement module comprising six three-axis fluxgates (Type MAG-03 from Bartington® Instruments) was constructed as shown in Fig. 2(a). To avoid interference between sensors and to enhance the gradient sensitivity, a separation $2x = 2y = 2z = 30$ cm between two fluxgates aligned along one of the coordinate axes was chosen. For instance, the $G_{xz}^{(m)}$ component is determined by taking the difference of B_x measured at the points $(0,0,-z)$ and $(0,0,z)$, divided by the distance, $2z$. As shown in Fig. 2(b), the measured $G_{xz}^{(m)}$ remained almost constant at a value of about

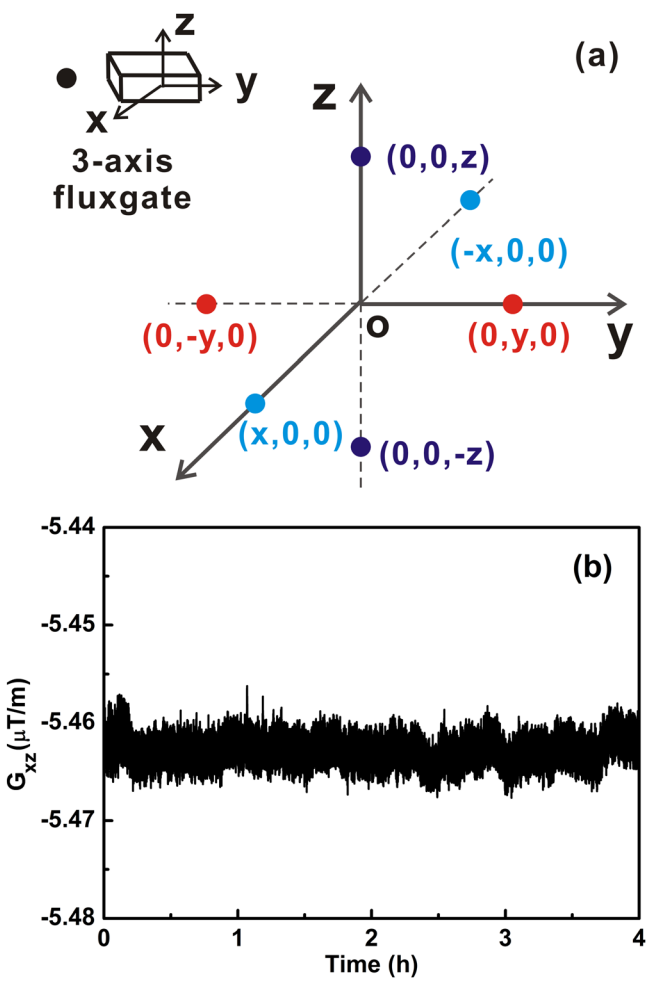

FIG. 2. (a) Fluxgate configuration for gradient field tensor detection. Six triaxial fluxgate units (18 fluxgates) are positioned at the indicated locations. (b) depicts the continuously measured environmental gradient field G_{xz} over 4 h time.

$-5.46\ \mu$T/m over a period of 4 h. This indicates that there is a good time correlation of the magnetic fields at the positions of the two fluxgates.[5]

Such gradient field will undoubtedly influence the MRI detection and cause the image distortion. One evidence is the NMR signal of two bottles of 6 ml water recorded in presence of environmental gradient fields. The two bottles were separated by 2.5 cm along the x axis, thus the G_{xx} of 4.38 μT/m caused a NMR peak splitting of about 5 Hz, but the peak heights differed. The $G^{(m)}$ tensor remains nearly constant during a quite long time, for example, one week or longer, indicating that the gradient field in our lab is mainly caused by the immobile magnetic sources, e.g., room walls, equipment nearby, etc.

Due to the geometrical constrictions imposed by the cryostat as well as the compactness and simplicity of the ULF MRI system, only six sets of gradient field coil pairs shown in Fig. 3(a) were used to compensate the environmental gradient field tensor. Besides the 3D imaging gradient coils, $G_{xx}^{(a)}$, $G_{xy}^{(a)}$, and $G_{xz}^{(a)}$, two more planar gradient coil pairs were used to produce $G_{yx}^{(a)}$ and $G_{yz}^{(a)}$. $G_{yy}^{(a)}$ was generated by the opposite connection of a pair of square Helmholtz coils. After applying the six gradient fields, all nine components of the final gradient tensor at the sample position were suppressed to be below the order of one μT/m. Please see the supplementary material for the analysis of the applied and concomitant tensors.[9]

To demonstrate the feasibility of the gradient field compensation method, the compensation effect was studied by recording the FID signals of two tap water samples mentioned above. First, the G_{xx} component was compensated by $G_{xx}^{(m)}$. In consequence, the two-peak NMR spectrum recovered to a single peak and the free induction decay (FID) signal of Fig. 3(b) lasted about 0.5 s. When the three imaging gradient fields were applied, the FID signal duration in Fig. 3(c) was extended to 1.0 s, corresponding to a linewidth of about 1.6 Hz. After all the six gradient coil pairs were utilized for compensation, the FID signal in Fig. 3(d) reached more than 2.5 s, 5 times longer than that compensated with only G_{xx}. In order to check if more directions of compensation are needed, the multi-echo train of this water sample, the grey trace in Fig. 3(d), was recorded to calculate the T_2 time with the Carr-Purcell-Meiboom-Gill (CPMG) pulse sequence. Six π pulses were excited after the $\pi/2$ pulse with time intervals of 300 ms. It is clearly seen that the envelope of the compensated FID almost touches that of the echo train. This means that the compensation result already comes close to the optimal situation. The corresponding linewidth of 0.76 Hz meets the requirement for MRI experiments.

In order to test the effect of the gradient compensation, 2D MRI experiments were performed using the filtered back-projection approach. A winter melon, an Asian vegetable, was chosen as the sample. It was carved into an O-shape with outer diameter of 4 cm and inner diameter of 2 cm. A photo is shown in the inset of Fig. 4(a). For this symmetric sample, the direction of the gradient field was rotated from 0° to 180° in 12 steps. The gradient field strength was 23.5 μT/m. Both FID and spin echo were recorded with averaging up to 25 times for each projection, see Fig. 4(a). We reconstructed the images with different numbers of averages,

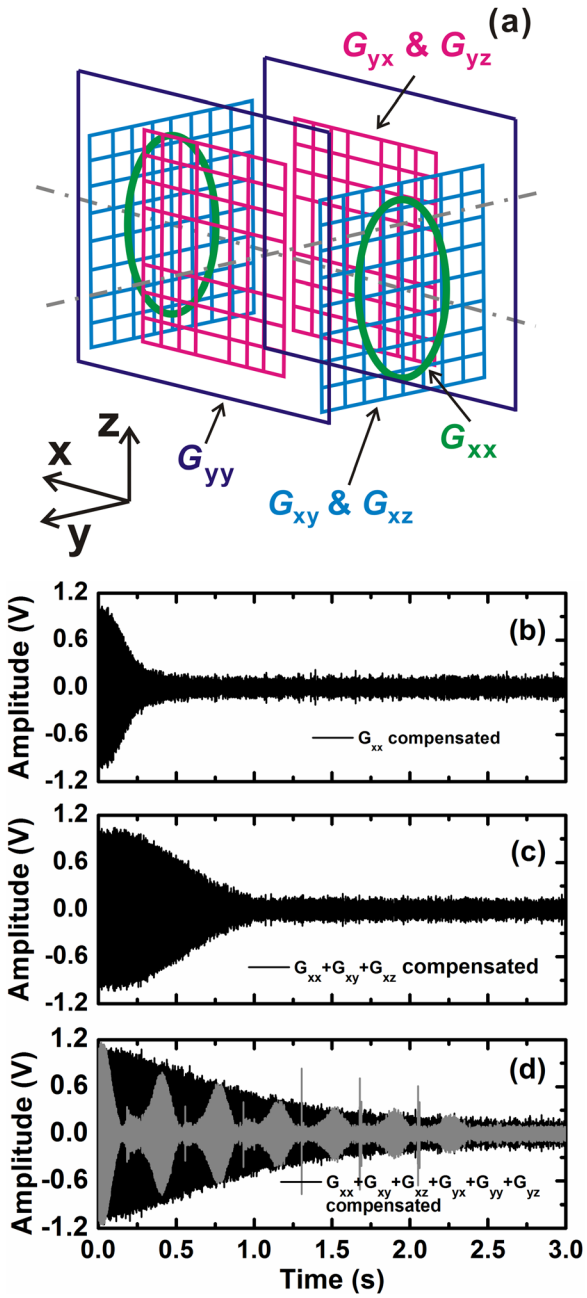

FIG. 3. (a) The gradient compensation coil system. It consists of 6 sets of coil pairs generating $G_{xx}^{(a)}$, $G_{xy}^{(a)}$, $G_{xz}^{(a)}$, $G_{yx}^{(a)}$, $G_{yy}^{(a)}$, and $G_{yz}^{(a)}$; (b) and (c) the FID signals with G_{xx} and $G_{xx}+G_{xy}+G_{xz}$ applied; (d) the FID signal (the black trace) obtained after all six components are compensated, and the multi-echo train (the gray line) recorded without gradient compensation. All the FID signals were averaged 5 times.

single shot, 10 averages, and 25 averages, as depicted in Figs. 4(b) and 4(c). In the single-shot image, the sample contour can be already recognized, but the image is partly distorted because of the noise. When the averaging number is increased, the imaging quality is evidently enhanced. The total imaging time for acquiring a 25-times averaged image was about 100 min, nearly 60% of which was the prepolarizing time.

Another advantage of gradient compensation was also demonstrated. In the experiments, the samples were polarized with a permanent magnet pair. The signal-to-noise ratio is significantly increased as compared to polarization by

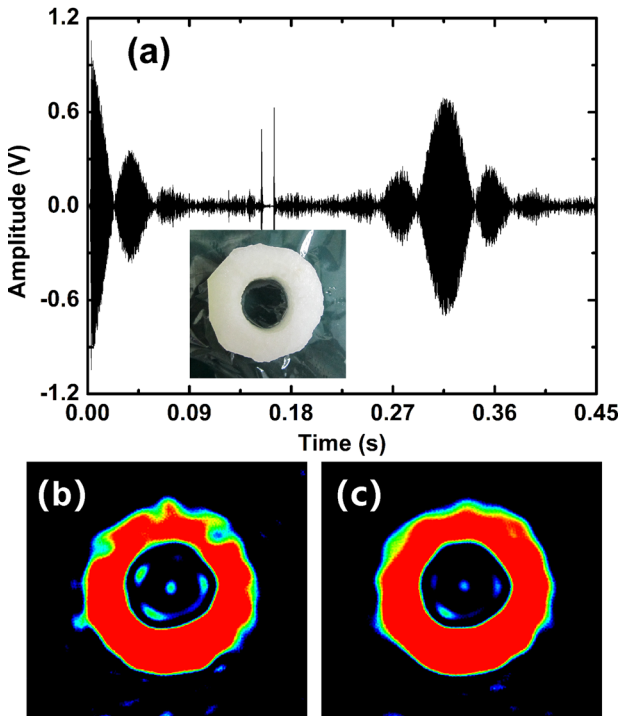

FIG. 4. (a) FID and spin echo signals of a slice of winter melon. The number of averages is 25. The inset shows a photo of the sample, with outer diameter of 4 cm and inner diameter of 2 cm. The MRI images reconstructed from echo signals are depicted: (b) single shot and (c) 25 times averaged.

electromagnets.[10] However, the leakage of magnetic field lines will cause an additional gradient field which may affect the B_m homogeneity. Therefore, the magnet pair was protected by the soft iron yoke and set 1.5 m away from the SQUID sensor. After introducing the gradient field compensation method, a reduction of the distance between magnet and SQUID was possible. We moved the magnet 1 m closer to the sensor, so the distance was only 0.5 m. The duration of the FID signal of the two-bottle water sample still can be compensated to be about 2 s (Fig. 5). The inset of Fig. 5 shows its FID signal without gradient field compensation. Note that the sample transporting time is shortened from 1.42 s to 0.8 s. The transporting time can be further decreased by either decreasing the magnet-sample distance

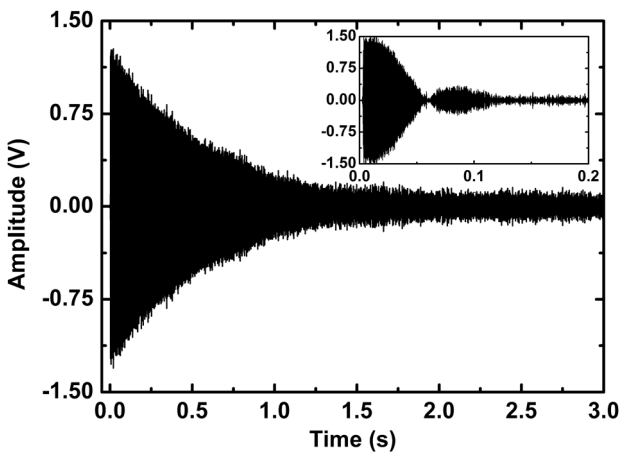

FIG. 5. The FID signal of two-bottle water sample with sample-magnet distance of 0.5 m. The inset is its FID signal without gradient field compensation.

or increasing the transporting speed. Therefore, the permanent magnet polarization method should be suitable for samples with a short transverse relaxation time T_2 sample utilizing gradient field compensation.

In conclusion, a gradient tensor detecting and compensating system was demonstrated to be effective for ULF NMR/MRI without magnetic shielding. NMR water signals with a linewidth of 0.76 Hz and 2D MRI images were recorded with low-T_c second-order gradiometer. With this gradient field compensation method, an inexpensive ULF NMR/MRI system can be realized for biological samples.

The authors thank Alex I. Braginski for helpful discussions and critical reading of the manuscript. This work was supported in part by the International Cooperation Project of Chinese Academy of Sciences (CAS) (Project No. GJHZ1104), collaborating with Forschungszentrum Jülich (FZJ), and by the projects from the National Natural Science Foundation of China (Grant No. 11204339), and from the Natural Science Foundation of Shanghai (Grant No. 12ZR1452900).

[1]J. Clarke and A. I. Braginski, *The SQUID Handbook* (WILEY-VCH, Weinheim, 2006), Vol. II.
[2]M. Moessle, S.-I. Han, W. Myers, S. K. Lee, N. Kelso, M. Hatridge, A. Pines, and J. Clarke, J. Magn. Reson. **179**, 146 (2006).
[3]S. K. Lee, M. Moessle, W. Myers, N. Kelso, A. H. Trabesinger, A. Pines, and J. Clarke, Magn. Reson. Med. **53**, 9 (2005).
[4]V. S. Zotev, A. N. Matlashov, P. L. Volegov, I. M. Savukov, M. A. Espy, J. C. Mosher, J Gomez, and R. H. Kraus, Jr., J. Magn. Reson. **194**, 115 (2008).
[5]L. Q. Qiu, C. Liu, H. Dong, L. Xu, Y. Zhang, H.-J. Krause, and X. M. Xie, Phys. Procedia **36**, 388 (2012).
[6]R. H. Koch, G. A. Keefe, and G. Allen, Rev. Sci. Instrum. **67**, 230 (1996); P. Schmidt, D. Clark, K. Leslie, M. Bick, D. Tilbrook, and C. Foley, Explor. Geophys. **35**, 297 (2004); R. Stolz, V. Zakosarenko, M. Schulz, A. Chwala, L. Fritzsch, H.-G. Meyer, and E. O. Koestlin, The Leading Edge **25**, 178 (2006).
[7]Y. Zhang, H. Soltner, H.-J. Krause, E. Sodtke, W. Zander, J. Schubert, M. Gruneklee, D. Lomparski, M. Banzet, H. Bousack, and A. I. Braginski, IEEE Trans. Appl. Supercond. **7**, 2866 (1997).
[8]C. Liu, Y. Zhang, L. Q. Qiu, H. Dong, H.-J. Krause, X. M. Xie, and A. Offenhaeusser, Supercond. Sci. Technol. **25**, 075013 (2012).
[9]See supplementary material at http://dx.doi.org/10.1063/1.4795516 for the analysis of the applied and concomitant tensors.
[10]H. Dong, Y. L. Wang, S. L. Zhang, Y. Sun, and X. M. Xie, Supercond. Sci. Technol. **21**, 115009 (2008).